

Preparation and Photochemical Behavior of Organoruthenium Derivatives of Photochromic Dithienylethene (DTE): DTE-(RRuL_m)_n (RRuL_m = (η⁶-C₆H₅)Ru(η⁵-C₅Me₅), (η⁶-C₆H₅)RuCl₂(PPh₃), (η⁵-C₅Me₄)Ru(CO)₂; n = 1, 2)[†]

Kazunori Uchida, Akiko Inagaki, and Munetaka Akita*

Chemical Resources Laboratory, Tokyo Institute of Technology, R1-27, 4259 Nagatsuta, Midori-ku, Yokohama 226-8503, Japan

Received May 31, 2007

A series of organoruthenium complexes containing photochromic 1,2-di(2-methylthien-3-yl)-3,3,4,4,5,5-hexafluorocyclopentene fragments (DTE), DTE-(RRuL_m)_n (RRuL_m = (η⁶-C₆H₅)Ru(η⁵-C₅Me₅) (**I**): n = 1 (**3**), 2 (**4**); (η⁶-C₆H₅)RuCl₂(PPh₃) (**II**): n = 1 (**10**), 2 (**11**); (η⁵-C₅Me₄)Ru(CO)₂ (**III**): n = 1 (**25**), 2 (**24**); substituted at the 5-position of the thiophene ring), are prepared and characterized by ¹H NMR and UV–vis spectroscopy, and molecular structures of the 1:2 adducts **4**, **11**, and **24** are determined by X-ray crystallography, which reveals the antiparallel conformation of the two thiophene rings suitable for photocyclization, causing the photochromism. It is revealed that the metalated DTE derivatives show photochromic behavior through the photochemical, electrocyclic conrotatory ring-closing and -opening processes in a manner analogous to the organic counterparts, but the efficiency of the photochromic processes is dependent on the attached metal fragments. The cationic Cp*Ru(η⁶-arene)-type (**I**) and neutral Cp*Ru(CO)₂Cl-type complexes (**III**) show photochromic behavior (content of the closed isomers at the UV photostationary states: 25–88%), and subsequent visible light irradiation of the equilibrated mixtures reverts the process to afford the open forms quantitatively. The ring-closing and -opening processes are reversible and can be repeated without notable deterioration. As for the series of Ph derivatives of **I** (**1**, **3**, and **4**), metalation improves the efficiency of the ring-closing process. In contrast to these derivatives, no significant photochromic behavior is noted for the benzo-fused derivatives of **I**, and UV irradiation of **II** (**10** and **11**) causes irreversible dissociation of the arene ligand (DTE).

Introduction

Photochromic compounds have attracted increasing attention, because various physicochemical properties of them, in particular, color, can be switched by the action of electromagnetic radiation and/or heat in a reversible manner.¹ Diarylethenes constitute a class of efficient photochromic compounds and exhibit such behavior through reversible, photochemical ring opening–closing processes.² A number of diarylethene derivatives were prepared and their photochemical properties were examined. Among them, 1,2-di(heteroaryl)ethenes, in particular, 1,2-di(2-methylthien-3-yl)-3,3,4,4,5,5-hexafluorocyclopentene derivatives developed by Irie (Scheme 1), turned out to show excellent photochromic properties superior to other derivatives with respect to many aspects such as fatigue resistance, quick response, high quantum yield, and reversibility.³

[†] This paper is dedicated to the late Professor Yoshihiko Itoh, not only an outstanding chemist but also a great mentor of science and life.

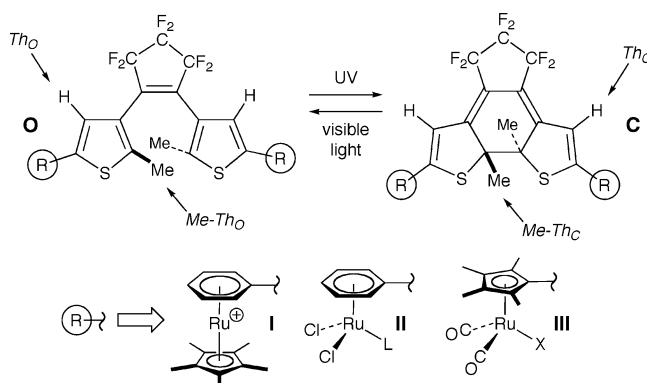
* To whom correspondence should be addressed. Fax: +81-45-924-5230. E-mail: makita@res.titech.ac.jp.

(1) Bamfield, P. *Chromic Phenomena, Technological Applications of Color Chemistry*; RSC: Cambridge, 2001. Dürr, H.; Bouas-Laurent, H. *Photochromism: Molecules and Systems*; Elsevier: Amsterdam, 2003. The special thematic issue of *Chem. Rev.* for “Photochromism: Memories and Switches—Introduction”, *Chem. Rev.* **2000**, *100*, 1683–1890. *Organic Photochromic and Thermochromic Compounds*; Crano, J. C., Guglielmetti, R. J., Eds.; Main Photochromic Families; Plenum Press: New York, 1999; Vol. 1.

(2) Kellogg, R. M.; Groen, M. B.; Wynberg, H. *J. Org. Chem.* **1967**, *32*, 3093.

(3) Irie, M. *Chem. Rev.* **2000**, *100*, 1683. Tian, H.; Yang, S. *Chem. Soc. Rev.* **2004**, *33*, 85.

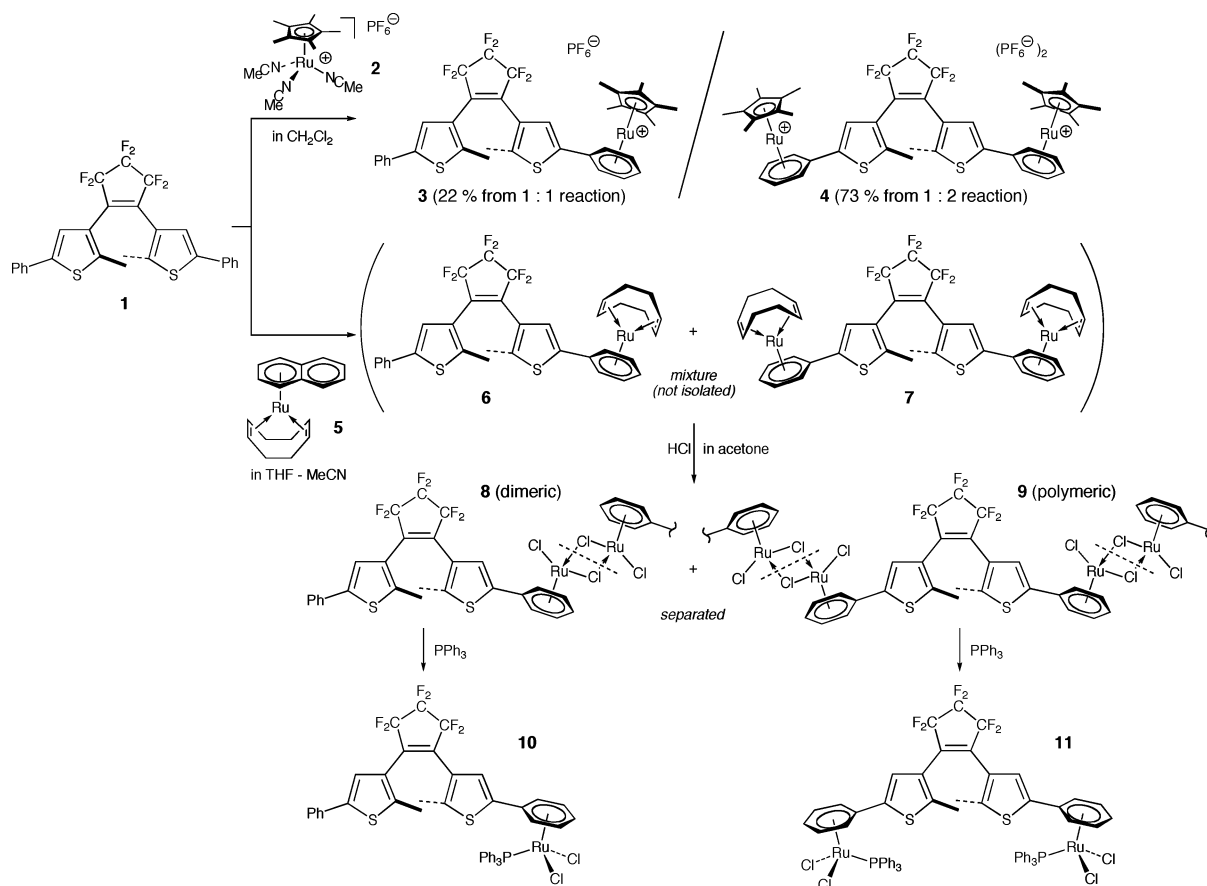
Scheme 1



The dithienylethene (DTE) derivatives exhibit photochromic behavior through the processes shown in Scheme 1. The colorless open form **O** containing the cross-conjugated π -system is converted, upon UV irradiation, to the closed form **C**, where the π -conjugated system is extended over the molecule to show an absorption in the visible region. The electrocyclic conrotatory ring-closing process can be reverted by visible light irradiation. The change of the conjugated system induces not only the color change but also a significant change of the electronic structure of the DTE part.

Combination of the chromic properties with other chemical auxiliaries would lead to a new phase of the chemistry, and various attempts have been made to add more sophisticated functions.³ If a metallic fragment is attached to the chromic

Scheme 2



molecule, the different forms of the chromic compounds with the different colors (i.e., different electronic structures) would show distinctive coordination properties, which turn on and off the functions unique to the attached metallic species (e.g., catalysis).^{3–5} From this viewpoint, we have been studying introduction of organometallic fragments to chromic compounds such as photochromic spiropyranes and halochromic pH indicators.⁶ Herein we describe the synthesis and photochromic behavior of three types of DTE–ruthenium complexes bearing the η^6 -arene and η^5 -cyclopentadienyl functional groups **I–III** (Scheme 1).

Results and Discussion

Preparation and Characterization of Dithienylethene–Ruthenium Complexes. The three types of ruthenium complexes prepared in the present study were the η^6 -arene-coordinated diphenyl–DTE compounds containing the cationic $\text{Ru}(\eta^5\text{-C}_5\text{Me}_5)$ (**I**) and neutral $\text{RuCl}_2(\text{L})$ fragments (**II**) and the η^5 -cyclopentadienyl complexes (**III**) (Scheme 1).

(i) Cationic (η^6 -DTE) RuCp^* -Type Complexes (I**).**⁷ The **I**-type, cationic η^6 -arene-coordinated complexes **3** and **4** were readily prepared by ligand displacement reactions of the labile acetonitrile adduct $[\text{Cp}^*\text{Ru}(\text{NCMe})_3]\text{PF}_6$, **2**,⁸ with DTE-Ph₂, **1** (Scheme 2). The 1:1 (**3**) and 1:2 adducts (**4**) were obtained in a selective manner by adjusting the **1**/2 ratio. The obtained products were characterized by spectroscopic and crystallographic methods. As a typical example, a ¹H NMR spectrum of **4** is shown in Figure 1a (UV 0 h). (For the abbreviations for the assigned signals, see Scheme 1). The η^6 -Ph coordination

(4) (a) Gilat, S. L.; Kawai, S. H.; Lehn, J.-M. *J. Chem. Soc., Chem. Commun.* **1993**, 1439. (b) Gilat, S. L.; Kawai, S. H.; Lehn, J.-M. *Chem.–Eur. J.* **1995**, *1*, 275. (c) Fernández-Acebes, A.; Lehn, J.-M. *Adv. Mater.* **1998**, *10*, 1519. (d) Takeshita, M.; Irie, M. *Chem. Lett.* **1998**, 1123. (e) Chen, B. Z.; Wang, M. Z.; Wu, Y. Q.; Tian, H. *Chem. Commun.* **2002**, 1060. (f) Tian, H.; Chen, B. Z.; Tu, H.; Müllen, K. *Adv. Mater.* **2002**, *14*, 918. (g) Peter, A.; McDonald, R.; Branda, N. R. *Chem. Commun.* **2002**, 2274. Ahmed, S. A. *J. Phys. Org. Chem.* **2002**, *15*, 392. (h) Liang, Y.; Dvornikov, A. S.; Rentzepis, P. M. *J. Mater. Chem.* **2003**, *13*, 286. (i) Yam, V. W.-W.; Ko, C.-C.; Zhu, N. *J. Am. Chem. Soc.* **2004**, *126*, 12734. (j) Jukes, R. T. F.; Adamo, V.; Hartl, F.; Belser, P.; De Cola, L. *Inorg. Chem.* **2004**, *43*, 2779. (k) Odo, Y.; Matsuda, K.; Irie, M. *Chem.–Eur. J.* **2006**, *12*, 4283. (l) Ahmed, S. A. *J. Phys. Org. Chem.* **2006**, *19*, 402. (m) Ko, C.-C.; Kwok, W. M.; Yam, V. W.-W.; Phillips, D. L. *Chem.–Eur. J.* **2006**, *12*, 5840. (n) Lee, P. H.-M.; Ko, C.-C.; Wong, K. M.-C.; Zhu, N.; Yam, V. W.-W. *Organometallics* **2007**, *26*, 15. (o) Lee, P. H.-M.; Ko, C.-C.; Zhu, N.; Yam, V. W.-W. *J. Am. Chem. Soc.* **2007**, *129*, 6058.

(5) Spirobenzopyrane complexes: ref 6a. Miyashita, A.; Iwamoto, A.; Kuwayama, T.; Shitara, H.; Aoki, Y.; Hirano, M.; Nohira, H. *Chem. Lett.* **1997**, 965. Atabekyan, L. S.; Chibisov, A. K. *J. Photochem.* **1986**, *34*, 323. Kimura, K.; Yamashita, T.; Yokoyama, M. *J. Chem. Soc., Perkin Trans. 2* **1992**, 613. Atabekyan, L.; Chibisov, A. *Mol. Cryst. Liq. Cryst. Sci. Tech., Sect. A* **1994**, *246*, 263. Atabekyan, L. S.; Lilikin, A. I.; Zakharova, G. V.; Chibisov, A. K. *High Energy Chem.* **1996**, *30*, 409. Kimura, K.; Teranishi, T.; Yokoyama, M. *Supramol. Chem.* **1996**, *7*, 11. Filley, J.; Ibrahim, M. A.; Nimlos, M. R.; Watt, A. S.; Blake, D. M. *J. Photochem. Photobiol., A: Chem.* **1998**, *117*, 193. Gerner, H.; Chibisov, A. K. *J. Chem. Soc., Faraday Trans.* **1998**, *94*, 2557. Collins, G. E.; Choi, L.-S.; Ewing, K. J.; Michelet, V.; Bowen, C. M.; Winkler, J. D. *Chem. Commun.* **1999**, 321. Kimura, K.; Sakamoto, H.; Kado, S.; Arakawa, R.; Yokoyama, M. *Analyst* **2000**, *125*, 1091. Nakamura, M.; Fujioka, T.; Sakamoto, H.; Kimura, K. *New J. Chem.* **2002**, *26*, 554. Bulanov, A. O.; Luk'yanov, B. S.; Kogan, V. A.; Stankevich, N. V.; Lukov, V. V. *Russ. J. Coord. Chem.* **2002**, *28*, 46. Querol, M.; Bozic, B.; Salluce, N.; Belser, P. *Polyhedron* **2003**, *22*, 655. Liu, S. *Mol. Cryst. Liq. Cryst.* **2004**, *419*, 97. Kimura, K.; Sakamoto, H.; Uda, M. *Macromolecules* **2004**, *37*, 1871. Azobenzene complex: Nishihara, H. *Coord. Chem. Rev.* **2005**, *249*, 1468, and references therein. See also a recent example: Tang, H.-S.; Zhu, N.; Yam, V. W.-W. *Organometallics* **2007**, *26*, 22. Dihydropyrene complexes: Mitchell, R. H.; Brkic, Z.; Sauro, V. A.; Berg, D. J. *J. Am. Chem. Soc.* **2003**, *125*, 7581. Zhang, R.; Fan, W.; Twamley, B.; Berg, D. J.; Mitchell, R. H. *Organometallics* **2007**, *26*, 1888.

(6) (a) Moriuchi, A.; Uchida, K.; Inagaki, A.; Akita, M. *Organometallics* **2005**, *24*, 6382. (b) Takano, K.; Inagaki, A.; Akita, M. *Chem. Lett.* **2006**, *35*, 434. (c) Hirasaka, M.; Inagaki, A.; Akita, M. *J. Organomet. Chem.* **2007**, *692*, 93.

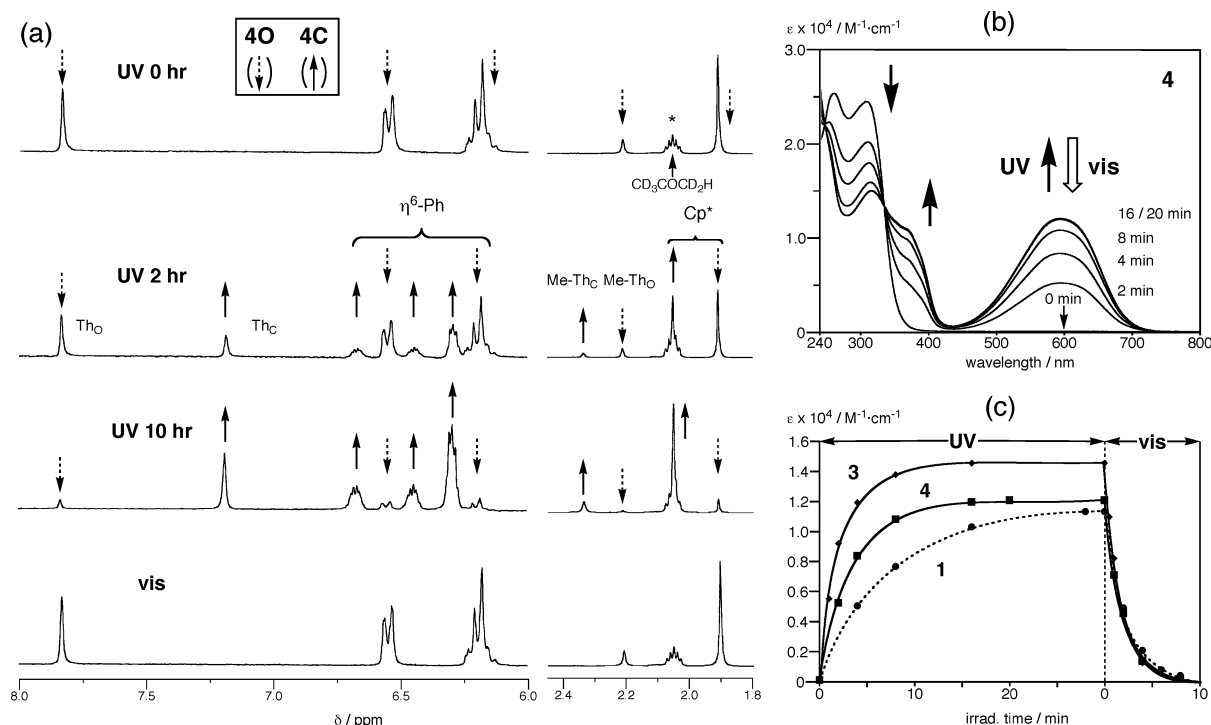
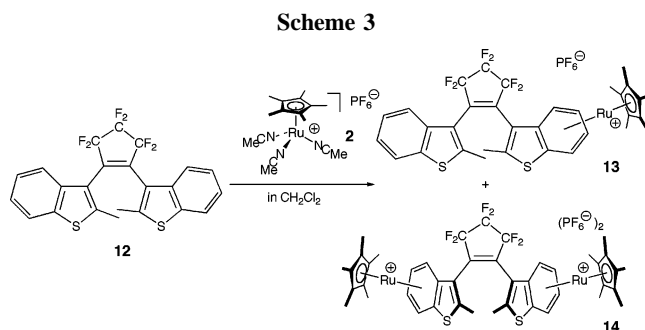


Figure 1. Spectral changes upon UV and vis light irradiation of **1–4**. (a) ^1H NMR spectral changes of **4** upon UV light irradiation (observed in acetone- d_6). (b) UV–vis spectral changes of **4** upon UV light irradiation (observed in CH_2Cl_2 ; $[\mathbf{4}] = 2.49 \times 10^{-5} \text{ M}$). (c) Visible absorption changes of **1–4** upon UV and vis light irradiation. The absorptions were monitored at the maxima of the visible absorptions (**1O**: 589 nm; **3O**: 600 nm; **4O**: 594 nm).

was confirmed by the upfield shift of the $\eta^6\text{-Ph}$ signals (^1H NMR; 7.3–7.6 \rightarrow 6.1–6.6).⁸ The ^1H NMR data for **4** indicate a symmetrical structure, whereas a ^1H NMR spectrum of the 1:1 adduct **3** contained two sets of the shifted and nonshifted signals (Figure S2; UV 0 h). The open (**O**) and closed forms (**C**) of the DTE part can be readily discriminated by a couple of spectroscopic features such as (i) the appearance of a visible absorption for **C**³ and (ii) the ^1H NMR signal for the methyl groups attached to the thiophene rings ($\delta_\text{H}(\text{Me-Th})$) (Scheme 1)); that is, the Me-Th_C signal appears in the lower field compared to that of the Me-Th_O signal.^{4a} For **4**, no absorption was observed in the visible region (Figure 1b; 0 min), and the Me-Th signal (^1H NMR; Figure 1a, 0 h) appeared in the higher field compared to that of the closed form, as will be discussed later. Similar features were noted for **3**, indicating that the thermal metal complexation (Scheme 2) of the open DTE molecule **1** gave the adducts **3** and **4** with retention of the open structure. The open structure of the 1:2 adduct **4** was also verified by X-ray crystallography (Figure 2a), and details will be discussed later.

The benzo-fused derivatives **13** and **14** were also prepared as references in a manner similar to the synthesis of **3** and **4** (Scheme 3). While they showed spectroscopic features similar to those of the Ph derivatives, formation of two conformational isomers was noted for **13** (ca. 6:4) as also observed for **12**. The dinuclear adduct **14** contained only one isomer. It is established



that (1) two isomers are feasible for the open form of DTE, i.e., antiparallel (**O**) and parallel conformers (**O'**), (2) the two conformers interconvert with each other, and (3) only the antiparallel isomer **O** undergoes the conrotatory photocyclization leading to the closed isomer (**C**) (Scheme 4).³ The two species of **12** and **13** were then assigned to the two conformers of the open form **O** and **O'**. Preliminary X-ray crystallography for the 1:2 adduct **14**⁹ revealed that the two benzothiophene rings in **14** were arranged in a parallel fashion **O'** in contrast to the antiparallel arrangement **O** observed for the other derivatives described in this paper (see below).

(ii) Neutral ($\eta^6\text{-DTE}$) $\text{RuCl}_2(\text{PPh}_3)$ -Type Complexes (II**).** Because the ($\eta^6\text{-arene}$) RuCp^* fragment included in the above-mentioned complexes **3** and **4** was known to be rather sluggish with respect to its chemical reactivity, we attempted introduction of a more functionalizable ruthenium unit such as ($\eta^6\text{-arene}$) $\text{RuCl}_2(\text{L})$.

Of a few methods established for synthesis of ($\eta^6\text{-arene}$) $\text{RuCl}_2(\text{L})$ -type complexes,¹⁰ we chose chlorination of the Ru(0) -

(7) See, for example: (a) Fagan, P. J.; Ward, M. D.; Calabrese, J. C. *J. Am. Chem. Soc.* **1989**, *111*, 1698. (b) Schrenk, J. L.; McNair, A. M.; McCormick, F. B.; Mann, K. R. *Inorg. Chem.* **1986**, *25*, 3501. (c) He, X. D.; Chaudret, B.; Dahan, F.; Huang, Y.-S. *Organometallics* **1991**, *10*, 970. (d) Vichard, D.; Gruselle, M.; Amouri, H. E.; Jaouen, G.; Vaissermann, J. *Organometallics* **1992**, *11*, 976. (e) Seiders, T. J.; Baldrige, K. K.; O'Connor, J. M.; Siegel, J. S. *J. Am. Chem. Soc.* **1997**, *119*, 4781. (f) Pasch, R.; Koelle, U.; Ganter, B.; Englert, U. *Organometallics* **1997**, *16*, 3950. (g) Steinmetz, B.; Schenk, W. A. *Organometallics* **1999**, *18*, 943.

(8) Kündig, E. P. *Transition Metal Arene π -Complexes in Organic Synthesis and Catalysis*; Springer: Berlin, 2004.

(9) Crystallographic data for **14**: formula: $\text{C}_{43}\text{H}_{44}\text{F}_{18}\text{P}_2\text{S}_2\text{Ru}_2$, monoclinic, space group $P2_1/c$, $a = 15.96(4) \text{ \AA}$, $b = 21.95(5) \text{ \AA}$, $c = 16.19(3) \text{ \AA}$, $\beta = 72.68(9)^\circ$, $V = 5414(19) \text{ \AA}^3$, $d = 1.510 \text{ g}\cdot\text{cm}^{-3}$. Current R value = 0.20. An ORTEP view is shown in Figure S6.

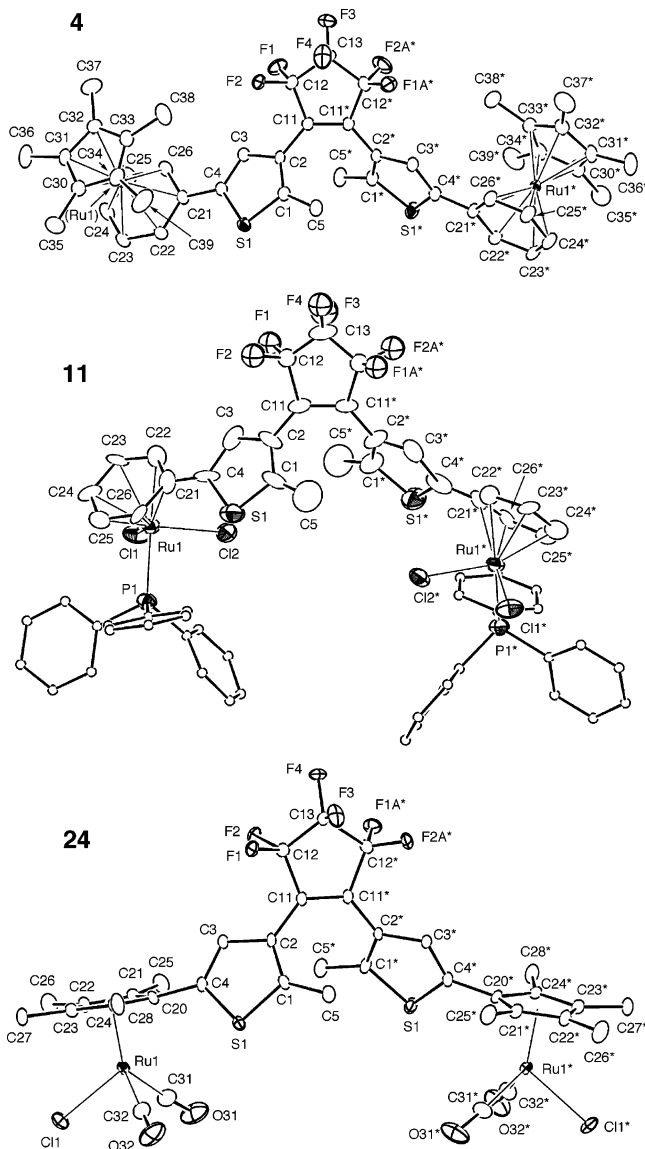
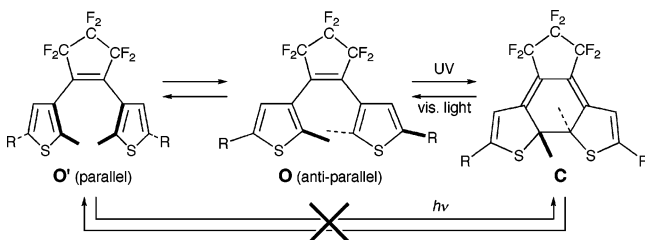


Figure 2. ORTEP views of the DTE-ruthenium complexes **4** (the cationic part), **11**, and **24** drawn with thermal ellipsoids at the 30% probability level.

Scheme 4

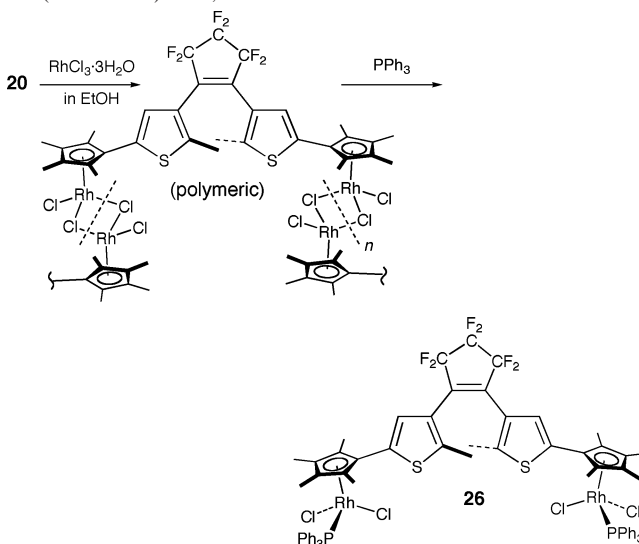


(η^6 -arene)(cod) precursor (Scheme 2). Treatment of the labile $\text{Ru}(\eta^6\text{-naphthalene})(\eta^4\text{-cod})$ complex **5**¹¹ with **1** in a THF–MeCN mixed solvent gave a mixture of the 1:1 (**6**) and 1:2 adducts (**7**) of the (η^6 -arene) $\text{Ru}(0)(\text{cod})$ intermediates, which

was inseparable and unstable to the air and, then, was subjected to chlorination with aqueous HCl. The obtained chlorinated brown products **8** and **9** were separated by taking advantage of their different solubilities. The dimeric 1:1 adduct **8** was soluble in acetone, whereas the 1:2 adduct **9** was slightly soluble in acetone presumably because of its polymeric structure. Subsequent treatment of **8** and **9** with PPh_3 readily gave the desired red, monomeric (η^6 -arene) $\text{RuCl}_2(\text{PPh}_3)$ -type products **II** (**10** and **11**), respectively. The η^6 -arene complexes **8**–**11** were readily characterized on the basis of the spectroscopic features as described for the Cp^* derivatives **3** and **4**.¹⁰ The η^6 -arene coordination was confirmed by the upfield shift of the coordinated η^6 -Ph signals (^1H NMR; for **10**, see the spectrum for 0 h in Figure 3a; the data for **11** are shown in Figure S3). Incorporation of PPh_3 in **10** and **11** was confirmed by the ^{31}P NMR signals, which were comparable to the signal reported for (η^6 -arene) $\text{RuCl}_2(\text{PPh}_3)$.¹⁰ The η^6 -arene complexes **8**–**11** contained the open DTE ligand as revealed by their UV–vis and ^1H NMR features, as discussed for **3** and **4**, and the open structure of the 1:2 adduct **11** was confirmed crystallographically (Figure 2b; see below).

(iii) (DTE- η^5 -C₅Me₄)Ru(CO)₂Cl-Type Complexes (III).¹² As described below, the η^6 -arene coordination in **II** (**10** and **11**) turned out to be so labile under UV irradiation as to undergo dissociation of the arene moiety, and then, we examined the synthesis of the η^5 -cyclopentadienyl derivative **24**, which should be more resistant to photodissociation (Scheme 5). Because the functionalized cyclopentadiene **20** was not reported, we designed its synthetic route as summarized in Scheme 5.¹³ The 1:1 adduct **25** was also prepared as a reference via **21**. Selective lithiation of 3,5-dibromo-2-methylthiophene **15** with $n\text{-BuLi}$ followed by treatment with tetramethylcyclopentenone **16** and acidic workup gave the 5-C₅Me₄H-substituted 3-bromo-2-methylthiophene **17**.¹⁴ Perfluorocyclopentene derivatives are known to be susceptible to nucleophilic substitution at the $=\text{C}-\text{F}$ moieties.¹⁵

(12) The related η^5 -C₅R₅-type Rh complex **26** was also prepared following the procedures reported for the η^5 -C₅Me₅ derivative (Kang, J. W.; Moseley, K.; Maitlis, P. M. *J. Am. Chem. Soc.* **1969**, *91*, 5970). Successive treatment of **20** with $\text{RhCl}_3 \cdot 3\text{H}_2\text{O}$ (in refluxing methanol) and PPh_3 (in diethyl ether at r.t.) gave **26** as red powder, which was characterized spectroscopically. In a manner similar to **12** and **13**, UV light irradiation of **26** caused appearance of a weak UV–vis shoulder band around 600 nm, which disappeared upon subsequent visible light irradiation (Figure S8), while no apparent change was detected by ^1H NMR. **26**: $\delta_{\text{H}}(\text{CDCl}_3)$ 7.60 (14H, br, Ph), 7.35 (8H, br, Ph), 7.23 (8H, br, Ph), 7.11 (2H, s, Th), 2.08 (6H, s, Me–Th), 1.54 (12H, d, $J = 4.6$, C₅Me₄), 1.37 (12H, d, $J = 2.7$, C₅Me₄). ^{31}P NMR (CDCl_3): 24.9 (d, $J_{\text{Rh-P}} = 143$). UV–vis (CH_2Cl_2) $\lambda_{\text{max}}/\text{nm}$ ($\epsilon/\text{M}^{-1}\text{cm}^{-1}$): 419, 280 nm.



(10) Werner, H.; Werner, R. *Chem. Ber.* **1982**, *115*, 3766. Bennett, M. A.; Smith, A. *J. Chem. Soc., Dalton Trans.* **1974**, 3011. Bennett, M. A.; Huang, T.-N.; Matheson, T. W.; Smith, A. K. *Inorg. Synth.* **1982**, *21*, 74. Bennett, M. A.; Neumann, H.; Thomas, M.; Wang, X. Q.; Pertici, P.; Salvadori, P.; Vitulli, G. *Organometallics* **1991**, *10*, 3237.

(11) Albers, M. O.; Ashworth, T. V.; Oosthuizen, H. E.; Singleton, E. *Inorg. Synth.* **1989**, *26*, 68. Powell, P. J. *Organomet. Chem.* **1974**, *65*, 89. See also ref 10.

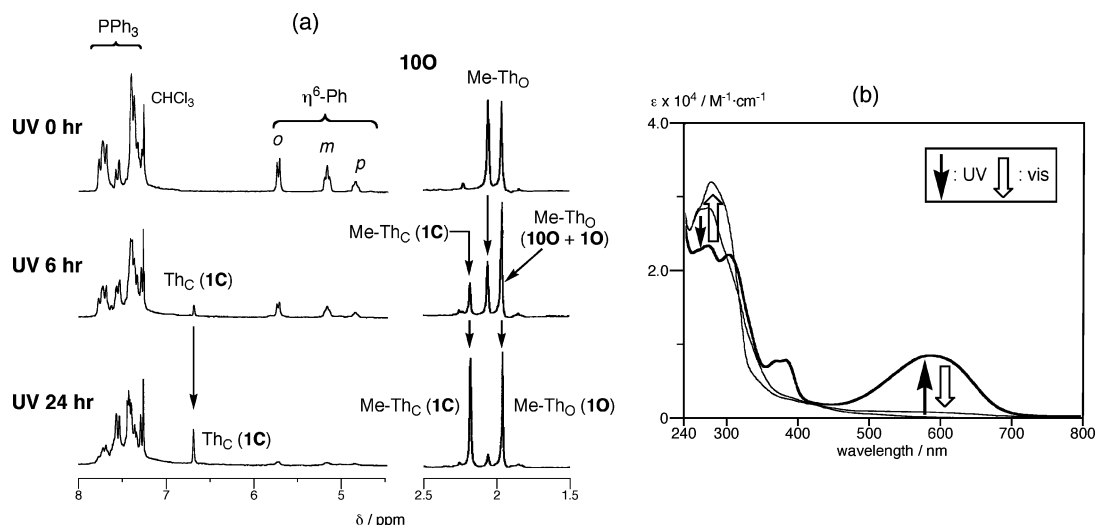
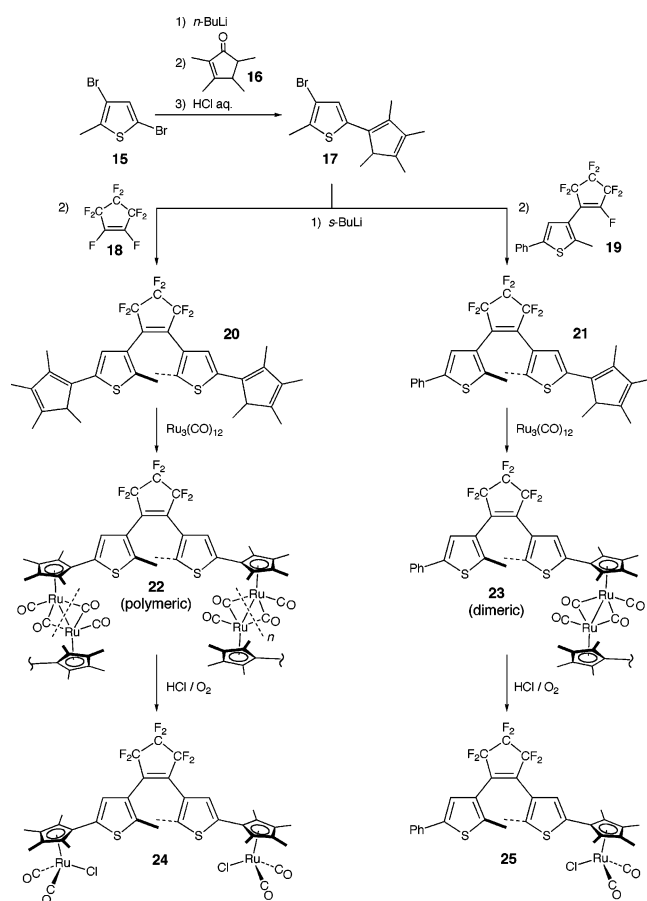


Figure 3. Spectral changes of **10** upon UV and visible light irradiation. (a) ^1H NMR spectral changes (observed in CDCl_3). (b) UV–vis NMR spectral changes (observed in CH_2Cl_2 : $[\mathbf{10}] = 2.18 \times 10^{-5} \text{ M}$).

Scheme 5



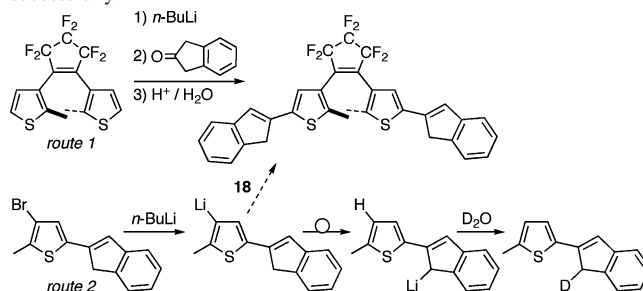
Lithiation of **17** with *s*-BuLi and subsequent treatment with the appropriate perfluorocyclopentene derivatives **18/19** gave the bis- (**20**) and mono-tetramethylcyclopentadiene derivatives (**21**), respectively, which were converted to the $(\eta^5\text{-C}_5\text{R}_5)\text{Ru}(\text{CO})_2\text{-Cl}$ -type complexes **24/25** according to the conventional methods, i.e., metalation with $\text{Ru}_3(\text{CO})_{12}$ followed by aerobic oxidative chlorination with $\text{HCl}(\text{aq})$.^{16,17}

The $(\eta^5\text{-C}_5\text{Me}_4)\text{Ru}(\text{CO})_2$ parts in **22/23** and **24/25** showed spectroscopic features similar to those of the corresponding Cp* derivatives, $\text{Cp}^*\text{Ru}_2(\text{CO})_4$ and $\text{Cp}^*\text{Ru}(\text{CO})_2\text{Cl}$, respectively.¹⁶ For example, the $\nu(\mu\text{-CO})$ absorptions observed for **22/23** disappeared upon chlorination, and instead two $\nu(\eta^1\text{-CO})$ bands

appeared. A ^1H NMR spectrum of **24** is shown in Figure 4a (UV 0 h). The open DTE structures in **22–25** were confirmed by their spectroscopic features (no visible absorption and $\delta_{\text{H}}(\text{Me-ThO})$), as discussed for **3** and **4**, and, for the 1:2 adduct **24**, by X-ray crystallography (Figure 2c).

(iv) **X-ray Crystallography of the DTE–Ruthenium Complexes 4, 11, and 24 (1:2 Adducts).** Molecular structures of the three 1:2 adducts **4**, **11**, and **24** were verified by X-ray crystallography. ORTEP views and selected structural parameters are shown in Figure 2 and Table 1, respectively. The three molecules are imposed on the crystallographic C_2 axis, leading to disorder of the central C_5F_6 ring. The structural parameters including the $\text{C1}\cdots\text{C1}^*$ separations as well as the dihedral angles between the perfluorocyclopentene's olefin part and the thiophene ring ($\angle\text{C1-C2-C11-C11}^*$: $45\text{--}51^\circ$) are similar and comparable to those of the nonmetalated derivative **1**,¹⁸ indicating that linking the bulky organometallic fragments does not cause significant conformational changes of the central DTE parts. On the other hand, the dihedral angles between the thiophene

(13) Preparation of a less sterically hindered indenyl derivative was attempted as shown below but unsuccessful. Via route 1, the desired product was formed but could not be separated from a mixture containing the mono-indenyl compound and the starting compound. For route 2, although the intermediate corresponding to **17** could be obtained, subsequent lithiation with *n*-BuLi was followed by proton-transfer to give the debrominated product, as confirmed by D_2O quenching. The less acidic $\text{C}_5\text{Me}_4\text{-H}$ proton in **17** was resistant to the proton transfer, and therefore, **20** was obtained successfully.



(14) Fendrick, C. M.; Schertz, L. D.; Mintz, E. A.; Marks, T. J.; Bitterwolf, T. E.; Horine, P. A.; Hubler, T. L.; Sheldon, J. A.; Belin, D. D. *Inorg. Synth.* **1992**, 29, 193.

(15) Hanazawa, M.; Sumiya, R.; Horikawa, Y.; Irie, M. *J. Chem. Soc., Chem. Commun.* **1992**, 206.

(16) Humphries, A. P.; Knox, S. A. R. *J. Chem. Soc., Dalton Trans.* **1975**, 1710. Knox, S. A. R.; Morris, M. J. *Inorg. Synth.* **1990**, 28, 189. Nagashima, H.; Mukai, K.; Shiota, Y.; Yamaguchi, K.; Ara, K.; Fukahori, T.; Suzuki, H.; Akita, M.; Moro-oka, Y.; Itoh, K. *Organometallics* **1990**, 9, 799.

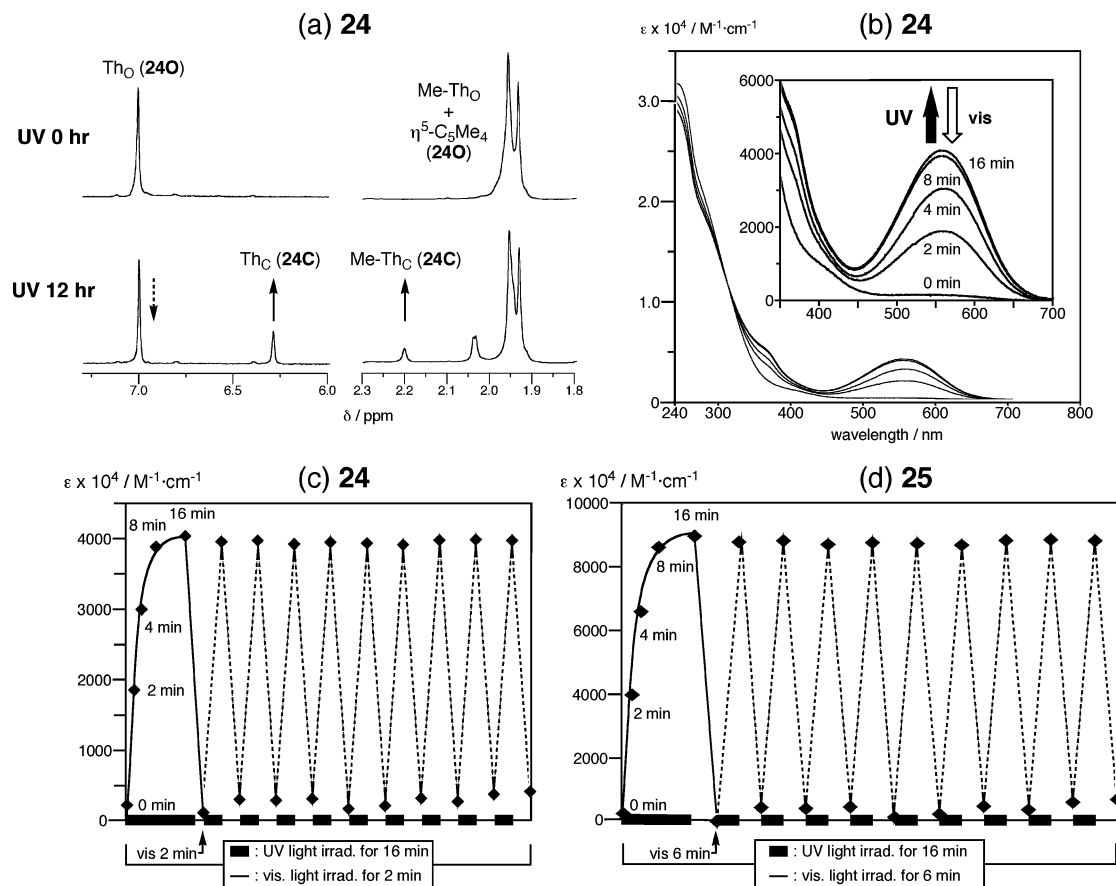


Figure 4. Spectral changes of **24** and **25** upon UV and visible light irradiation. (a) ^1H NMR spectral changes of **24** (observed in CD_2Cl_2). (b) UV–vis spectral changes of **24** (observed in CH_2Cl_2 ; $[\mathbf{24}] = 2.50 \times 10^{-5} \text{ M}$). (c) Reversible photochromism of **24** monitored by UV–vis spectroscopy ($[\mathbf{24}] = 2.60 \times 10^{-5} \text{ M}$; alternating UV (16 min) and visible light (2 min) irradiations). (d) Reversible photochromism of **25** monitored by UV–vis spectroscopy ($[\mathbf{25}] = 2.50 \times 10^{-5} \text{ M}$; alternating UV (16 min) and visible light (6 min) irradiations). For c and d, only the final absorbances are shown from the second cycle.

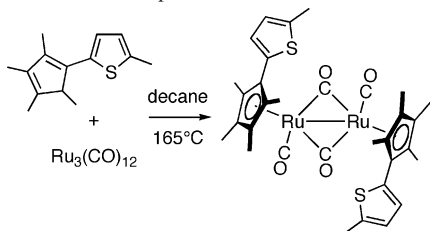
ring and the attached aromatic rings (Ph and $\eta^5\text{-C}_5\text{R}_5$) are dependent on the attached metal fragments. As for the phenyl derivatives **4** and **11** ($\angle\text{C3}–\text{C4}–\text{C21}–\text{C22} < 18^\circ$), the arrangements of the phenyl rings with respect to the thiophene rings are closer to a coplanar one, to lead to extension of the π -conjugated system to some extent. On the other hand, the 2,5-dimethyl substituents on the $\eta^5\text{-C}_5\text{Me}_4$ rings in **24** hinder such an orientation, and as a result, the C_5Me_4 rings are twisted

with respect to the thiophene rings, as indicated by the substantially large dihedral angle ($\angle\text{C3}–\text{C4}–\text{C20}–\text{C21}$: $57.4(6)^\circ$).

As for the conformation of the two thiophene rings (Scheme 4), the three DTE complexes **4**, **11**, and **24** adopt the antiparallel conformation **O**, as is evident from the ORTEP views (Figure 2), whereas the two benzothiophene rings in **14** are arranged in a parallel fashion **O'**, as revealed by the preliminary X-ray crystallography (Figure S6).⁹ The two different conformations affect the efficiency of the photochemical processes as described below and as pointed out by the previous studies.¹⁹

The structural features of the organoruthenium moieties are essentially the same as those of the corresponding counterparts, e.g., $[\text{Cp}^*\text{Ru}(\eta^6\text{-C}_6\text{H}_6)]^-$,²⁰ $(\eta^6\text{-C}_6\text{H}_6)\text{RuCl}_2(\text{PPh}_3)$,²¹ and $\text{Cp}^*\text{Ru}(\text{CO})_2\text{Cl}$.²² The C–C distances of the η^6 -coordinated Ph parts in **4** and **11** are elongated compared to the free arene **1** owing to the back-donation from the Ru centers.⁸

(17) Because the thiophene part may participate in the reaction with $\text{Ru}_3(\text{CO})_{12}$, a preliminary experiment using a simpler thiophene-containing substrate was carried out and the expected product was obtained successfully and characterized spectroscopically (δ_H (CDCl_3) 6.99, 6.72 (2H \times 2, m \times 2, Th), 2.49 (6H, s, Me-Th), 1.95, 1.77 (12H \times 2, s \times 2, C_5Me_4); IR (CH_2Cl_2) 1932, 1763 cm^{-1}). But attempted preparation of the $\text{Cp}^*\text{RuCl}(\text{PPh}_3)_2$ -type complex by successive treatment of the simpler thiophene with $\text{RuCl}_3 \cdot n\text{H}_2\text{O}$ (in refluxing EtOH) and PPh_3 resulted in the formation of a small amount of unidentified products.



(18) Irie, M.; Lifka, T.; Kobatake, S.; Kato, N. *J. Am. Chem. Soc.* **2000**, *122*, 4871. See also: Yamada, T.; Muto, K.; Kobatake, S.; Irie, M. *J. Org. Chem.* **2001**, *66*, 6164.

(19) Uchida, K.; Nakayama, Y.; Irie, M. *Bull. Chem. Soc. Jpn.* **1990**, *63*, 1311. Irie, M.; Miyatake, O.; Uchida, K.; Eriguchi, T. *J. Am. Chem. Soc.* **1994**, *116*, 9894. Takeshita, M.; Yamada, M.; Kato, N.; Irie, M. *J. Chem. Soc., Perkin Trans. 2* **2000**, 619. Yamaguchi, T.; Fujita, Y.; Nakazumi, H.; Kobatake, S.; Irie, M. *Tetrahedron* **2004**, *60*, 9863.

(20) See, for example, the $[\text{Cp}^*\text{RuBr}_3]^-$ salt: Gemel, G.; Mereiter, K.; Schmid, R.; Kirchner, K. *Organometallics* **1996**, *15*, 532. See also ref 7.

(21) Elsegood, M. R. J.; Tocher, D. A. *Polyhedron* **1995**, *14*, 3147.
(22) Fan, L.; Turner, M. L.; Adams, H.; Bailey, N. A.; Maitlis, P. M. *Organometallics* **1995**, *14*, 676. Knowles, D. R. T.; Adams, H.; Maitlis, P. M. *Organometallics* **1998**, *17*, 1741. Martin-Matute, B.; Edin, M.; Bogar, K.; Kaynak, F. B.; Backvall, J.-E. *J. Am. Chem. Soc.* **2005**, *127*, 8817.

Table 1. Selected Structural Parameters for the Diruthenium Complexes **4**, **11**, and **24**^a

| | 4 | 11 ^b | 24 ^c | 1 ^d |
|---|----------------|------------------------|------------------------|-----------------------|
| Interatomic Distances | | | | |
| S1–C1 | 1.719(3) | 1.71(2) | 1.721(4) | 1.715(5) |
| S1–C4 | 1.731(3) | 1.75(2) | 1.727(4) | 1.727(5) |
| C1–C2 | 1.370(4) | 1.42(3) | 1.383(5) | 1.374(7) |
| C1–C5 | 1.497(6) | 1.52(3) | 1.486(5) | 1.498(7) |
| C2–C3 | 1.432(5) | 1.41(3) | 1.454(5) | 1.422(6) |
| C2–C11 | 1.470(4) | 1.41(2) | 1.451(5) | 1.449(6) |
| C3–C4 | 1.361(4) | 1.43(3) | 1.350(6) | 1.346(6) |
| C4–C21 | 1.472(5) | 1.42(3) | 1.479(5) ^e | 1.471(7) |
| C11–C11* | 1.351(6) | 1.44(3) | 1.353(8) | 1.343(6) |
| C11–C12 | 1.504(4) | 1.52(4) | 1.510(5) | 1.493(7) |
| C12–C13 | 1.515(4) | 1.47(4) | 1.46(2) | 1.500(7) |
| C1–C1* | 3.593(5) | 3.63(5) | 3.906(8) | 3.507(3) |
| C–C in Ph | 1.396–1.422(5) | 1.35–1.41(3) | | 1.348–1.380(7) |
| Ru–C(Ph) | 2.209–2.234(4) | 2.13–2.27(2) | | |
| C–C in η^5 -C ₅ R ₅ | 1.415–1.428(6) | | 1.407–1.448(8) | |
| C–Me in η^5 -C ₅ R ₅ | 1.497–1.507(7) | | 1.473–1.526(8) | |
| Ru–C(η^5 -C ₅ R ₅) | 2.166–2.186(3) | | 2.192–2.258(5) | |
| Bond Angles | | | | |
| C1–S1–C4 | 92.9(2) | 96(1) | 93.0(2) | 93.1(2) |
| S1–C1–C2 | 110.6(3) | 109(2) | 110.6(3) | 110.4(4) |
| S1–C1–C5 | 119.4(2) | 119(2) | 120.3(3) | 120.0(4) |
| C2–C1–C5 | 130.0(3) | 132(2) | 129.1(4) | 129.5(5) |
| C1–C2–C3 | 112.9(2) | 113(2) | 112.1(3) | 112.1(4) |
| C1–C2–C11 | 123.7(3) | 121(2) | 125.1(3) | 124.7(4) |
| C3–C2–C11 | 123.2(2) | 126(2) | 122.8(3) | 123.3(4) |
| C2–C3–C4 | 113.2(3) | 114(2) | 113.0(3) | 114.6(4) |
| S1–C4–C3 | 110.4(3) | 107(2) | 111.3(3) | 109.7(4) |
| S1–C4–C21 | 120.6(2) | 128(1) | 121.8(3) ^f | 121.5(4) |
| C3–C4–C21 | 129.0(3) | 125(2) | 126.9(3) ^g | 128.8(5) |
| C2–C11–C11* | 129.3(2) | 130(1) | 128.9(2) | 129.2(4) |
| C2–C11–C12 | 119.8(2) | 125(2) | 120.3(4) | 120.8(4) |
| C4–C21–C22 | 119.9(2) | 123(2) | 126.3(4) | 121.3(5) |
| C4–C21–C26 | 121.4(3) | 114(2) | 124.8(3) | 123.1(5) |
| Dihedral Angles | | | | |
| C1–C2–C11–C11* | 45.6(5) | 51(4) | 45.7(6) | 48.5(5) |
| C3–C4–C21–C22 | 5.4(4) | 18(3) | 57.4(6) ^h | 15.7(5) |

^a Interatomic distances in Å and bond and dihedral angles in deg. ^b Ru1–C11: 2.374(5), Ru1–C12: 2.385(5), Ru1–P1: 2.344(4). ^c Ru1–C11: 2.400(1), Ru1–C31: 1.888(6), Ru1–C32: 1.899(5), O1–C31: 1.129(8), O2–C32: 1.120(6). ^d Ref 18. ^e C4–C20. ^f C4–C20–C21. ^g C4–C20–C24. ^h C3–C4–C20–C21.

Photochromic Behavior of the DTE Complexes. The photochromic behavior of the obtained DTE–Ru complexes was examined by means of UV–vis and ¹H NMR spectroscopy as compared with the free DTE molecule **1**. UV and visible light irradiation was performed with a high-pressure mercury lamp ($\lambda < 360$ nm) and a Xe lamp ($\lambda > 420$ nm), respectively, with appropriate cutoff filters.

(i) **Cationic (η^6 -Arene)RuCp* Complexes I (3 and 4).** ¹H NMR and UV–vis spectral changes of **4** brought about upon UV and visible light irradiation are shown in Figure 1, and the data for **1** and **3** are included in the Supporting Information (Figures S1 and S2).²³

UV irradiation of a CH₂Cl₂ solution of **4** caused a color change to purple. The change was followed by UV–vis spectroscopy (Figure 1b), and the intensities of the absorption maximum (594 nm) are plotted as a function of the irradiation time as shown in Figure 1c. After irradiation for 16 min the system reached a photostationary state, which, upon subsequent visible light irradiation, was reverted to the original state within 10 min. The change was also followed by ¹H NMR (Figure 1a). UV light irradiation caused the appearance of a set of new signals with the disappearance of the signals for **4C**. The new

species was assigned to the closed isomer **4C** on the basis of (1) the above-mentioned electronic absorption appearing in the visible region and (2) the Me–Th signal ($\delta_{\text{H}}(\text{Me–Th}_\text{C})$ 2.34; cf. $\delta_{\text{H}}(\text{Me–Th}_\text{O})$ 2.21).^{4a} After 10 h irradiation the system reached the photostationary state with the composition being as large as **4C/4O** = 88:12, and subsequent visible light irradiation completely replaced the signals for **4C** with those of **4O**. Thus the cationic (η^6 -arene)RuCp*-type complex **4** showed photochromic behavior originating from the ring-opening and -closing processes in a manner similar to the free DTE molecule **1**.²⁴ The photochemical electrocyclic processes were reversible, and no apparent deterioration of **4** was observed after repeating the processes several times. As can be seen from Figure 1a (¹H NMR), no decomposition product was detected for the sample after the visible light irradiation.

The purple closed isomer **4C** could be isolated from a **4C**-rich photoequilibrated mixture by column chromatography (eluted with CH₂Cl₂–MeOH, 100:1) and characterized by ¹H NMR ($\delta_{\text{H}}(\text{acetone-}d_6)$ 7.18 (2H, s, Th), 6.66, 6.44 (2H \times 2, m \times 2, *m*- and *m'*- η^6 -Ph), 6.29 (6H, m, *o*- and *p*- η^6 -Ph), 2.34 (6H, s, Me–Th), 2.05 (30H, s, Cp*).). Because the chiral, central part was fixed by the ring closure, the *m*- and *m'*- η^6 -Ph protons became inequivalent. The isolated closed isomer **4C** was stable in the dark.

(23) The different rates of the photochromic processes observed by ¹H NMR and UV–vis measurements should result from the different concentrations of the samples. In the case of the ¹H NMR sample of a higher concentration, light does not transmit the sample completely to make the photochemical process less efficient.

(24) Irie, M.; Lifka, T.; Kobatake, S.; Kato, N. *J. Am. Chem. Soc.* **2000**, *122*, 4871.

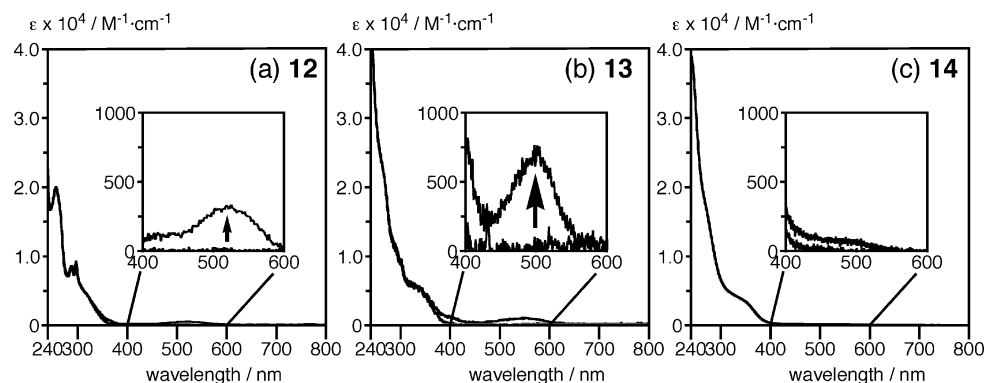


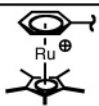
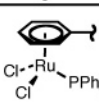
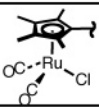
Figure 5. UV-vis spectral changes of **12** (a; [**12**] = 4.00×10^{-5} M), **13** (b; [**13**] = 1.07×10^{-5} M), and **14** (c; [**14**] = 2.13×10^{-5} M) upon UV light irradiation for 1 h (observed in CH_2Cl_2).

Similar behavior was noted for the 1:1 adduct **3** and the free DTE molecule **1** (Figures S1,2), and their UV-vis spectral changes are compared with that of **4** as shown in Figure 1c and Scheme 6.²⁵ As can be seen from Figure 1c, the ring-closing rates for the three species were comparable, but the metal complexes reached the photostationary states slightly faster than the free DTE molecule (ca. 16 min for **3** and **4** and ca. 30 min for **1**). No significant difference, however, was observed for the reverse ring-opening processes (within 10 min), which were faster than the ring-closing process. The metalation did not cause a notable shift of the absorption maxima of the closed isomers ($\lambda_{\text{max}}(\text{C})$: 589–600 nm) but affected the efficiency of the ring-closing process (Scheme 6). The metalation promoted the photochemical cyclization process, as can be seen from the O/C ratio at the UV photostationary state (from 43:57 (**1**) up to 12:88 (**4**)).

In order to see the effect of the thiophene unit, the benzo-fused derivative **12**²⁶ was also subjected to metalation and the desired 1:1 (**13**) and 1:2 adducts (**14**) were obtained successfully as described above. Although no ^1H NMR spectral change was observed at all upon UV irradiation (Scheme 6), UV-vis spectral monitoring revealed formation of very small amounts of the closed isomers for **12** and **13**, but the 1:2 adduct **14** turned out to be totally inert with respect to the photochemical conversion (Figure 5).²³ Preliminary X-ray crystallography of **14** (Figure S6) revealed the parallel conformation of the two benzothiophene rings, which hindered the photocyclization (Scheme 4).¹⁹ The benzo-fused derivative **12**, therefore, was not further subjected to the following metal complexation reactions.

(ii) Neutral (η^6 -Arene) $\text{RuCl}_2(\text{PPh}_3)_2$ Complexes **10 and **11** (II).** UV irradiation of **10** and **11** caused a color change to blue, suggesting photochromic behavior, and spectral changes induced by the UV irradiation are shown in Figures 3 and S3, respectively. However, it was concluded that complex **10** did not undergo reversible photochemical processes but irreversible decomposition, as is evidenced by (1) the disappearance of the upfield-shifted ^1H NMR signals for the η^6 -Ph part indicating dissociation of the Ph part from the Ru center, (2) the appearance of the ^1H NMR signals assignable to the open and closed

Scheme 6

| R^1 | R^2 | compd. | $\lambda_{\text{max}}(\text{C})$ / nm ^a | O : C ^b (UV photost. state) |
|---|--------------|-----------|---|---|
| Ph | | 1 | 589 | 43 : 57 ^{c,d} |
|  | Ph | 3 | 600 | 16 : 84 ^{c,e} |
| | | 4 | 594 | 12 : 88 ^{c,f} |
|  | Ph | 10 | decomposed ^d | |
| | | 11 | decomposed ^d | |
|  | Ph | 25 | 574 | 31 : 69 ^{c,g} |
| | | 24 | 556 | 75 : 25 ^{c,e} |
| BzTh ^h | | 12 | 523 ⁱ | ~100 : ~0 ^{d,i,j} |
| BzTh-Ru ^h | BzTh | 13 | 556 ⁱ | ~100 : ~0 ^{d,i,j} |
| | | 14 | - ^k | 100 : 0 ^{d,k} |

^a observed in CH_2Cl_2 . ^b determined by ^1H NMR. See also ref. 4a.

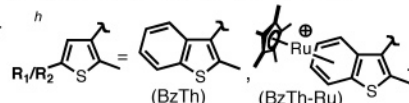
^c reverted to **O** upon visible light irradiation. ^d CDCl_3 . ^e CD_2Cl_2 .

^f acetone- d_6 . ^g C_6D_6 .

^h photochromism

detected by UV-vis.

ⁱ photochromism not detected by ^1H NMR. ^k photochromism not detected even by UV-vis.

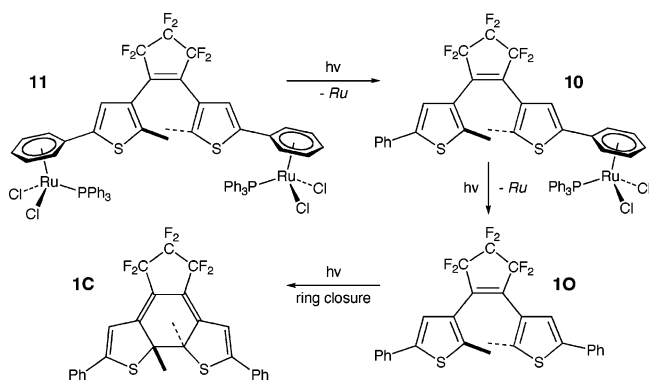


isomers of the free ligand **10**/C, and (3) the UV-vis spectrum obtained after visible light irradiation, being dissimilar to the original spectrum, in particular, in the UV region. The spectral changes observed for **10** are interpreted in terms of Scheme 7; UV irradiation caused the phenyl ligand dissociation rather than the ring closure to give the closed form of the free ligand **10**, which was subsequently converted to the closed isomer **1C** by the action of the UV light. The 1:2 adduct **11** followed the analogous decomposition pathway; that is, photolysis of **11** caused the phenyl ligand dissociation²⁷ to give the 1:1 adduct **10** (as detected by ^1H NMR; Figure S3), which underwent

(25) No significant solvent effect was noted, and the difference was within 5%; for example, **25O**/**25C** = 39:61 in CDCl_3 and **24O**/**24C** = 78:22 in CD_2Cl_2 . The results shown in Scheme 6 are for the solvent, in which the largest C/O ratios were observed. In the case of **4**, because the dicationic species was not soluble in CD_2Cl_2 enough for a ^1H NMR measurement, acetone- d_6 was used as the solvent.

(26) Kobatake, S.; Yamada, M.; Yamada, T.; Irie, M. *J. Am. Chem. Soc.* **1999**, *121*, 8450.

Scheme 7



further ligand dissociation to give the free, open (**10**) and then closed ligand (**1C**). Thus it was concluded that the blue coloration of the solutions of **11** is due to formation of **1C**, not due to formation of the closed isomers of **10** and **11**.

(iii) (η^5 -C₅R₅)Ru(CO)₂Cl Complexes **III** (**24** and **25**) and (η^5 -C₅R₅)RhCl₂(PPh₃) Complex **IV** (**27**). The photolabile nature of the (η^6 -arene)Ru complexes **10** and **12** described above prompted us to examine the derivative with the negatively charged η^5 -C₅R₅-type ligand. Photolysis of the 1:2 adduct **24** was followed by ¹H NMR and UV-vis spectroscopy²³ (Figure 4a,b; spectral changes for **25** are shown in Figure S4), which revealed photochromism of the Cp*Ru(CO)₂Cl-type complexes **24** and **25** similar to that observed for the cationic (η^6 -arene)RuCp* adducts **3** and **4** (**I**). The absorption maxima of the closed isomers **24C** and **25C** are higher in energy compared to the Ph derivatives **3** and **4** (Scheme 6), presumably because the π -conjugated system of the central DTE part is not extended to the η^5 -C₅R₅ rings owing to their considerably twisted arrangements with respect to the thiophene rings (see above).

It took ca. 16 min to reach the photostationary states, whereas the cycloreversion was completed within 2 (**24**) and 6 min (**25**). Thus the rates of cyclization of **24** and **25** were comparable to those of **3** and **4**, but the cycloreversion processes of **24** and **25** were slightly faster than those of **3** and **4**. The ring-opening efficiency of **24** and **25**, however, was inferior to that of **3** and **4** (Scheme 6), and only a quarter of the open 1:2 adduct **25O** was converted to the closed isomer **25C**.

Carbonylmetal complexes such as **24** and **25** may be prone to photochemical decarbonylation,²⁸ which may result in decomposition. The stability of **10** and **11** with respect to the photochemical decarbonylation process was examined by repeating the UV and visible light irradiation cycles, and the change of the intensity of the absorption maximum of the visible absorption was monitored by UV-vis spectroscopy. Because any notable deterioration was not observed, as can be seen from Figures 4c,d, the carbonylruthenium complexes **24** and **25** turned out to be fatigue-resistant up to at least ca. 10 times.

The difference between the electronic states of the open and closed forms was estimated by IR. Because **25O** was converted to the closed isomer more efficiently than **24O** (Scheme 6), the changes of the ν (CO) absorptions of **25** were monitored by IR. UV irradiation brought about shifts of the ν (CO) stretches from

2039 and 1988 cm⁻¹ to 2041 and 1991 cm⁻¹ (photostationary state) (Figure S7). The higher energy shifts indicate that the DTE moiety in the closed isomer **25C** is a better π -acceptor than that in the open form **25O** because of the extended π -conjugated system included in **25C**, but the extent of the shifts is not significant. This is because, as discussed above, the 2,5-methyl substituents of the η^5 -C₅Me₄ rings prevent a coplanar conformation. Such a twisted conformation should hinder effective electronic interaction between the central DTE part and the attached organometallic moieties.

Conclusions

Three types of organoruthenium complexes containing the photochromic DTE functional groups are prepared and characterized spectroscopically and crystallographically.

It is revealed that the metalated DTE derivatives show photochromic behavior through the photochemical, electrocyclic conrotatory ring-closing and -opening processes in a manner similar to the organic counterparts, but the efficiency of the photochromic processes is dependent on the attached metal fragments. The cationic Cp*Ru(η^6 -arene)-type (**I**) and neutral Cp*Ru(CO)₂Cl-type complexes (**III**) show photochromic behavior. UV light irradiation causes formation of equilibrated mixtures of the closed and open forms with C/O ratio of 25:75 to 88:12. Visible light irradiation of the equilibrated mixtures reverts the process to afford the open form **O** quantitatively, and the ring-closing and -opening processes can be repeated without notable deterioration even for the possibly photolabile carbonyl complexes such as **24** and **25** (up to ca. 10 times). As for the series of the Ph derivatives of **I** (**1**, **3**, and **4**), metalation improves the efficiency of the ring-closing process. The closed isomers of **I** and **III** turn out to be stable (at least for 24 h), when they are kept in the dark. In contrast to these derivatives, no significant photochromic behavior is noted for the benzo-fused derivatives of **I** (**12** and **13**), and UV irradiation of the neutral (η^6 -arene)RuCl₂(PPh₃)-type complexes **II** (**10** and **11**) causes irreversible dissociation of the arene ligand (DTE). The reason for the different photochemical properties of the DTE complexes is not clear at the moment: The steric repulsion in the closed form caused by the bulky metal fragments may be more severe than that in the open form. Many metal auxiliaries having absorptions in the visible region are also regarded as chromophores, and irradiation may excite not only the DTE part but also the metal auxiliaries to affect the photochromic properties. Further studies are needed to clarify these factors.

The change of the electronic properties at the metal centers induced by the photochromic process is estimated for the **III**-type complex **25** on the basis of the ν (CO) vibrations, and it is found that the change is not significant, presumably because the π -conjugated system of the central DTE moiety is not effectively extended to the η^5 -C₅Me₄ rings owing to the twisted arrangements of the η^5 -C₅Me₄ rings with respect to the thiophene rings. Studies targeting systems where the metallic auxiliaries can respond sensitively to the change of the DTE part (e.g., σ -bonded complexes: DTE-MLn) are now underway, and the results will be reported in due course.

Experimental Section

General Methods. All manipulations were carried out under an inert atmosphere by using standard Schlenk tube techniques. THF,

(27) See ref 8. See also: Dougan, S. J.; Melchart, M.; Habtemariam, A.; Parsons, S.; Sadler, P. J. *Inorg. Chem.* **2006**, *45*, 10882. Tudose, A.; Demonceau, A.; Delaude, L. *J. Organomet. Chem.* **2006**, *691*, 5356. Delaude, L.; Demonceau, A.; Noels, A. F. *Chem. Commun.* **2001**, 986. Cambie, R. C.; Clark, G. R.; Coombe, S. L.; Coulson, S. A.; Rutledge, P. S.; Wodgate, P. D. *J. Organomet. Chem.* **1996**, *507*, 1. Pearson, A. J.; Lee, K. J. *Org. Chem.* **1994**, *59*, 2304.

(28) Yamamoto, A. *Organotransition Metal Chemistry*; Wiley-Interscience: New York, 1986. Collman, J. P.; Hegedus, L. S.; Norton, J. R.; Finke, R. G. *Principles and Applications of Organotransition Metal Chemistry*, 2nd ed.; University Science Books: Mill Valley, CA, 1987; Crabtree, R. H. *The Organometallic Chemistry of the Transition Metals*, 4th ed.; Wiley-Interscience: New York, 2005.

diethyl ether (Na–K alloy), $\text{CH}_2\text{Cl}_2(\text{P}_2\text{O}_5)$, acetone (KMnO_4), and MeOH ($\text{Mg}(\text{OMe})_2$) were treated with appropriate drying agents, distilled, and stored under argon. ^1H and ^{13}C NMR spectra were recorded on Bruker AC-200 (^1H , 200 MHz) and JEOL EX-400 spectrometers (^1H , 400 MHz; ^{13}C , 100 MHz). Solvents for NMR measurements containing 0.5% TMS were dried over molecular sieves, degassed, distilled under reduced pressure, and stored under Ar. Coupling constants are reported in Hz. UV–vis and IR spectra (KBr pellets) were obtained on a JASCO V570 and FT/IR 5300 spectrometer, respectively. ESI-mass spectra were recorded on a ThermoQuest Finnigan LCQ Duo mass spectrometer. UV and visible light irradiations were performed with an Ushio high-pressure mercury lamp (UM-452; $\lambda < 360$ nm with a U-360 cutoff filter) and a Soma Kogaku Xe lamp (150 W; $\lambda > 420$ nm with an L42 cutoff filter), respectively. Elemental analyses were performed at the Center for Advanced Materials Analysis, Technical Department, Tokyo Institute of Technology. The organic compounds (**1**,²⁴ **12**,¹⁵ **15**,²⁹ and **19**³⁰) and the metal reagents (**2**,^{7g} **5**,¹¹ and $\text{Ru}_3(\text{CO})_{12}$ ³¹) were prepared following the published procedures. Other chemicals were purchased and used as received.

Preparation of 3. To a CH_2Cl_2 solution (10 mL) of **1** (232 mg, 0.446 mmol) cooled at -78°C was added slowly **2** (205 mg, 0.406 mmol) dissolved in CH_2Cl_2 (10 mL), and the resultant mixture was stirred for 2 h. Removal of the volatiles followed by chromatographic separation (alumina; eluted with CH_2Cl_2) gave **3** as a colorless powder (81 mg, 0.089 mmol, 22%). ^1H NMR (CDCl_3): δ 7.57 (2H, d, $J = 7.1$, *o*-Ph), 7.39 (2H, t, $J = 7.3$, *m*-Ph), 7.38 (1H, s, Th), 7.31 (1H, t, $J = 7.3$, *p*-Ph), 7.24 (1H, s, Th), 6.07 (2H, d, $J = 5.9$, *o*- η^6 -Ph), 6.00 (2H, t, $J = 5.7$, *m*- η^6 -Ph), 5.94 (1H, t, $J = 5.6$, *p*- η^6 -Ph), 2.04, 2.07 (3H \times 2, s \times 2, Me–Th), 1.82 (15H, s, Cp*). UV–vis (CH_2Cl_2) $\lambda_{\text{max}}/\text{nm}$ ($\epsilon/\text{M}^{-1}\text{cm}^{-1}$): 279 (3.03×10^4). ESI-MS: 757.6 ($\text{M}^+ - \text{PF}_6$). Anal. Calcd for $\text{C}_{37}\text{H}_{33}\text{F}_{12}\text{S}_2\text{PRu}$: C, 49.28; H, 3.69. Found: C, 48.96; H, 3.73.

Preparation of 4. A mixture of **1** (103 mg, 0.197 mmol) and **2** (302 mg, 0.599 mmol) dissolved in CH_2Cl_2 (20 mL) was stirred for 6 h. Removal of the volatiles followed by chromatographic separation (alumina; eluted with acetone) and crystallization from acetone–diethyl ether gave **4** as yellow crystals (185 mg, 0.144 mmol, 73%). ^1H NMR (acetone- d_6): δ 7.80 (2H, s, Th), 6.52 (4H, d, $J = 5.9$, *o*- η^6 -Ph), 6.19–6.12 (6H, m, *m*- and *p*- η^6 -Ph), 2.02 (6H, s, Me–Th), 1.89 (30H, s, Cp*). UV–vis (CH_2Cl_2) $\lambda_{\text{max}}/\text{nm}$ ($\epsilon/\text{M}^{-1}\text{cm}^{-1}$): 308 (2.46×10^4), 261 (2.54×10^4). ESI-MS: 1139.2 ($\text{M}^+ - \text{PF}_6$). Anal. Calcd for $\text{C}_{47}\text{H}_{48}\text{F}_{18}\text{P}_2\text{S}_2\text{Ru}_2$: C, 44.00; H, 3.77. Found: C, 43.91; H, 4.03.

Preparation of 8 and 9. **5** (1.27 g, 3.77 mmol) and **1** (0.92 g, 1.77 mmol) dissolved in THF (130 mL)–MeCN (1.3 mL) were stirred for 64 h, and then, the volatiles were removed under reduced pressure. The resultant mixture of **6** and **7** was subjected to chlorination without separation. The residue was dissolved in acetone (35 mL) and cooled at -78°C . To the mixture was added 36% HCl(aq) (2 mL) diluted with acetone (35 mL). The resultant mixture was stirred for 1 h at -78°C and for 1 h at room temperature. Addition of diethyl ether caused precipitation of **9** as a brown solid, which was washed with acetone (0.56 g, 0.63 mmol, 35%). The supernatant solution was evaporated, and dissolution of the residue in acetone followed by precipitation with diethyl ether gave **8** as a brown solid (0.59 g, 0.86 mmol, 48%). The crude samples of **8** and **9** were characterized spectroscopically and used without further purification. **8**: ^1H NMR ($\text{DMSO}-d_6$): δ 7.83 (1H, s, Th), 7.63 (2H, d, $J = 7.6$, *o*- η^6 -Ph), 7.46 (1H, s, Th), 7.42 (2H, t, $J = 7.3$, *m*-Ph), 7.33 (1H, t, $J = 7.2$, *p*-Ph), 6.36 (2H, d, $J = 5.4$, *o*- η^6 -Ph), 6.11 (2H, br, *m*- η^6 -Ph), 5.93 (1H, br, *p*- η^6 -Ph), 2.02, 1.99

(s \times 2, 3H \times 2, Me–Th). ESI-MS: 1349.0 (M^+ (dimer) – Cl). **9**: ^1H NMR ($\text{DMSO}-d_6$): δ 7.76 (2H, s, Th), 6.34 (4H, d, $J = 5.9$, *o*- η^6 -Ph), 6.11 (4H, d, $J = 5.5$, *m*- η^6 -Ph), 5.96 (2H, t, $J = 5.5$, *p*- η^6 -Ph), 2.04 (s, 6H, Me–Th). ESI-MS: 831.1 (M^+ (monomer) – 2Cl).

Preparation of 10. A CH_2Cl_2 solution (10 mL) of **8** (93 mg, 0.13 mmol) and PPh_3 (43 mg, 0.162 mmol) was stirred for 3.5 h. After removal of the volatiles the residue was subjected to chromatographic separation (alumina; eluted with THF). Precipitation from THF–pentane gave **10** as red powders (95 mg, 0.099 mmol, 74% based on crude **8**; 36% based on **1**). ^1H NMR (CDCl_3): δ 7.75–7.26 (22H, m, aromatic), 5.73 (2H, d, $J = 5.9$, *o*- η^6 -Ph), 5.19 (2H, t, $J = 5.1$, *m*- η^6 -Ph), 4.87 (1H, br, *p*- η^6 -Ph), 2.08, 1.99 (3H \times 2, s \times 2, Me–Th). ^{31}P NMR (CDCl_3): δ 21.6 (s). UV–vis (CH_2Cl_2) $\lambda_{\text{max}}/\text{nm}$ ($\epsilon/\text{M}^{-1}\text{cm}^{-1}$): 273 (2.46×10^4). ESI-MS: 956 (M^+). Anal. Calcd for $\text{C}_{46}\text{H}_{35}\text{F}_6\text{P}_2\text{S}_2\text{Cl}_4\text{Ru}$ (**10**· CH_2Cl_2 ; a sample obtained from CH_2Cl_2 –diethyl ether): C, 53.14; H, 3.39. Found: C, 53.46; H, 3.53.

Preparation of 11. The 1:2 adduct **9** (109 mg, 0.122 mmol) was treated with PPh_3 (83 mg, 0.32 mmol) as described for the synthesis of **10**. Similar workup and precipitation from THF–pentane gave **11** as red powders (119 mg, 0.0857 mmol, 79% based on crude **9**; 28% based on **1**). ^1H NMR (CDCl_3): δ 7.75–7.67 (12H, m, aromatic), 7.39–7.28 (20H, m, Ph), 5.73 (4H, d, $J = 5.9$, *o*- η^6 -Ph), 5.20–5.17 (4H, m, *m*- η^6 -Ph), 4.70 (1H, td, $J = 5.2$ and 2.2, *p*- η^6 -Ph), 2.24 (6H, s, Me–Th). ^{31}P NMR (CDCl_3): 22.0 (s). UV–vis (CH_2Cl_2) $\lambda_{\text{max}}/\text{nm}$ ($\epsilon/\text{M}^{-1}\text{cm}^{-1}$): 308 (2.68×10^4 , sh), 252 (4.65×10^4 , sh). ESI-MS: 1353.0 ($\text{M}^+ - \text{Cl}$), 1090.0 ($\text{M}^+ - \text{Cl} - \text{PPh}_3$). Anal. Calcd for $\text{C}_{63}\text{H}_{48}\text{F}_6\text{P}_2\text{S}_2\text{Cl}_4\text{Ru}_2$: C, 54.47; H, 3.48. Found: C, 54.25; H, 3.58.

Preparation of 13. To a CH_2Cl_2 solution (15 mL) of **12** (279 mg, 0.596 mmol) cooled at -78°C was added a CH_2Cl_2 solution (15 mL) of **2** (273 mg, 0.541 mmol) dissolved in CH_2Cl_2 (15 mL), and the resultant mixture was stirred for 1 h at the same temperature. After removal of the volatiles at room temperature under reduced pressure the residue was subjected to chromatography (alumina; eluted with THF). Precipitation of the obtained product from CH_2Cl_2 –diethyl ether gave **13** as a colorless solid (126 mmol, 0.148 mmol, 27%). ^1H NMR (acetone- d_6): δ Ar: 7.82 (1H, d, $J = 8.1$), 7.76–7.79 (1H, m), 7.69 (1H, br), 7.55 (1H, d, $J = 7.8$), 6.87 (1H, d, $J = 5.9$), 6.80 (1H, d, $J = 5.9$), 6.60 (1H, d, $J = 6.1$), 6.15 (1H, t, $J = 5.7$), 6.07 (1H, t, $J = 5.7$), 6.63 (1H, d, $J = 6.1$), 6.60 (1H, d, $J = 6.1$), 6.15 (1H, t, $J = 5.7$), 6.07 (1H, t, $J = 5.7$), 5.91 (1H, t, $J = 5.7$), 5.82 (1H, t, $J = 5.7$), 2.74, 2.58 (3H \times 2, s \times 2, Me–Th), 1.83 (15H, s, Cp*). UV–vis (CH_2Cl_2) $\lambda_{\text{max}}/\text{nm}$ ($\epsilon/\text{M}^{-1}\text{cm}^{-1}$): 330 (4.0×10^3 , sh). ESI-MS: 705.4 ($\text{M}^+ - \text{PF}_6$). Anal. Calcd for $\text{C}_{33}\text{H}_{29}\text{F}_{12}\text{P}_2\text{S}_2\text{Ru}$: C, 46.64; H, 3.44. Found: C, 46.28; H, 3.31.

Preparation of 14. A mixture of **12** (102 mg, 0.219 mmol) and **2** (320 mg, 0.634 mmol) dissolved in CH_2Cl_2 (15 mL) was stirred for 10 h. After removal of the volatiles under reduced pressure the residue was subjected to chromatography (alumina; eluted with MeCN). Extraction with THF followed by crystallization from CH_2Cl_2 –diethyl ether gave **14** as colorless powders (72 mg, 0.058 mmol, 27%). ^1H NMR (acetone- d_6): δ Ar: 6.83 (2H, d, $J = 5.9$), 6.62 (2H, d, $J = 5.9$), 5.97 (H, t, $J = 5.9$), 5.90 (2H, t, $J = 5.9$), 2.67 (6H, s, Me–Th), 1.80 (30H, s, Cp*). UV–vis (CH_2Cl_2) $\lambda_{\text{max}}/\text{nm}$ ($\epsilon/\text{M}^{-1}\text{cm}^{-1}$): 340 (4.1×10^3 , sh). ESI-MS: 1086.2 ($\text{M}^+ - \text{PF}_6$). Anal. Calcd for $\text{C}_{43}\text{H}_{44}\text{F}_{18}\text{P}_2\text{S}_2\text{Ru}_2$: C, 41.95; H, 3.60. Found: C, 41.50; H, 3.71.

Preparation of 17. To a THF solution (160 mL) of **15** (26.0 g, 102 mmol) cooled at -78°C was added *n*-BuLi (1.57 M, 70 mL, 110 mmol), and the resultant mixture was stirred for 20 min at the same temperature. After addition of a THF solution (120 mL) of **16** (18.0 mL, 120 mmol) the mixture was stirred for 28 h at room temperature. To the mixture was added water (200 mL) and concentrated HCl(aq) (200 mL) and stirred for 1 h. The acidic mixture was neutralized by Na_2CO_3 (aq), and the organic phase was

(29) Lantz, R.; Hörnfeldt, A. B. *Chem. Scr.* **1972**, 2, 9.

(30) Peters, A.; Vitols, C.; McDonald, R.; Neil R. Branda, N. R. *Org. Lett.* **2003**, 5, 1183.

(31) Bruce, M. I.; Jensen, C. M.; Jones, N. L. *Inorg. Synth.* **1990**, 28, 216.

Table 2. Crystallographic Data

| | 4 | 11 | 24 |
|--|--|--|--|
| solvent | (acetone) ₂ | (CH ₂ Cl ₂) ₂ | |
| formula | C ₅₃ H ₆₀ O ₂ F ₁₈ P ₂ S ₂ Ru ₂ | C ₆₅ H ₅₂ F ₆ P ₂ S ₂ Cl ₈ Ru ₂ | C ₃₇ H ₃₂ O ₄ F ₆ S ₂ C ₁₂ Ru ₂ |
| fw | 1399.23 | 1558.95 | 991.81 |
| cryst syst | monoclinic | monoclinic | monoclinic |
| space group | C2/c | P2 ₁ /n | C2/c |
| a/Å | 22.918(2) | 9.908(8) | 26.694(5) |
| b/Å | 16.0017(8) | 14.60(2) | 13.400(2) |
| c/Å | 17.421(2) | 22.54(3) | 13.509(3) |
| β/deg | 116.007(3) | 89.52(6) | 112.257(1) |
| V/Å ³ | 5741.9(8) | 3260(7) | 4472(1) |
| Z | 4 | 2 | 4 |
| d _{calcd} /g·cm ⁻³ | 1.618 | 1.588 | 1.473 |
| μ/mm ⁻¹ | 0.753 | 0.961 | 0.947 |
| no. of diffractions collected | 23 577 | 18 077 | 16 063 |
| no. of variables | 376 | 283 | 271 |
| R1 for data | 0.0444 | 0.0949 | 0.0626 |
| with I > 2σ(I) | (for 5716 data) | (for 1447 data) | (for 4549 data) |
| wR2 | 0.1309 | 0.2853 | 0.2237 |
| | (for all 6537 data) | (for all 6873 data) | (for all 5003 data) |

washed with water and dried over Na₂SO₄. Removal of the volatiles by a rotary evaporator followed by chromatographic separation (silica gel eluted with hexane) gave a mixture of **17** and a small amount of 3-bromo-2-methylthiophene, and the latter was removed under reduced pressure. The crude **17** (23.6 g, 79.4 mmol, 78%) was used without further purification. ¹H NMR (CDCl₃): δ 6.65 (1H, s, Th), 2.99 (1H, m, C₅Me₄H), 2.40 (3H, s, Th–Me), 2.08 (3H, d, J = 1.6, C₅Me₄), 1.91, 1.84 (3H × 2, s × 2, C₅Me₄), 1.11 (3H, d, J = 7.4, CHMe). FD–MS: 296 (M⁺).

Preparation of 20. To an ethereal solution (100 mL) of **17** (5.17 g, 17.4 mmol) cooled at –78 °C was added *n*-BuLi (0.98 M, 20 mL, 19.6 mmol), and the mixture was stirred for 30 min. Upon addition of the resultant mixture to an ethereal solution (100 mL) of **18** (1.20 mL, 8.94 mmol) cooled at 0 °C, the yellow solution turned to red. After the mixture was stirred for 3 h at 0 °C the reaction mixture was quenched with 1.2 N HCl(aq). The separated organic phase was washed with water and dried over Na₂SO₄. Chromatographic separation (silica gel) gave **20** (2.12 g, 3.48 mmol, 40% based on crude **17**; 32% based on **15**) as a green oil. ¹H NMR (CDCl₃): δ 6.76 (2H, s, Th), 3.02 (1H, d, J = 7.3, C₅Me₄H), 2.06, 1.96, 1.91, 1.84 (3H × 4, s × 4, C₅Me₄ and Me–Th), 1.08 (3H, d, J = 7.6, CHMe). FD–MS: 608 (M⁺).

Preparation of 21. To an ethereal solution (10 mL) of **17** (370 mg, 1.24 mmol) cooled at –78 °C was added *n*-BuLi (1.00 M, 1.4 mL, 1.4 mmol), and the mixture was stirred for 30 min. Upon addition of the resultant mixture to an ethereal solution (10 mL) of **19** (395 mg, 1.08 mmol) cooled at 0 °C, the yellow solution turned to red. The workup as described for **20** gave **21** (314 mg, 0.556 mmol, 44% based on crude **17**; 34% based on **15**) as a green oil. ¹H NMR (CDCl₃): δ 7.56–7.28 (6H, m, Ar), 6.76 (1H, s, Th), 3.04 (1H, m, C₅Me₄H), 2.06 (3H, s, C₅Me₄), 1.97 (3H, s, Me–Th), 1.08 (3H, d, J = 7.6, CHMe). FD–MS: 564 (M⁺). Anal. Calcd for C₃₀H₂₆F₆S₂: C, 63.81; H, 4.64. Found: C, 63.43; H, 4.91.

Preparation of 22. A mixture of **20** (1.12 g, 1.84 mmol) and Ru₃(CO)₁₂ (0.78 g, 1.22 mmol) suspended in decane (degassed by evacuation for a short period) was heated at 165 °C. The mixture turned into a red solution. After the mixture was left at room temperature for 1 day an orange precipitate appeared, which was collected and washed with pentane. Dissolution in THF followed by chromatographic separation (alumina) gave crude **22** (596 mg, 0.649 mmol, 35% based on Ru₃(CO)₁₂) as an orange solid. ¹H NMR (CDCl₃): δ 7.11 (2H, s, Th), 1.98 (6H, s, Me–Th), 1.95, 1.79 (6H × 2, s × 2, C₅Me₄). IR (KBr): 1938, 1763 cm⁻¹.

Preparation of 23. Treatment of **21** (296 mg, 0.53 mmol) with Ru₃(CO)₁₂ (123 mg, 0.293 mmol) as described for the synthesis of **22** gave crude **23** (332 mg, 0.230 mmol, 80% based on Ru₃(CO)₁₂) as an orange solid. ¹H NMR (CDCl₃): δ 7.55–7.28 (6H, m, Ph

and Th), 7.05 (1H, s, Th), 2.01, 1.92 (3H × 2, s × 2, Me–Th), 1.92, 1.77 (6H × 2, s × 2, C₅Me₄). IR (KBr): 1938, 1763 cm⁻¹.

Preparation of 24. Crude **22** (200 mg, 0.217 mmol) was dissolved in a mixture of CHCl₃ (3 mL), ethanol (1 mL), and 2 N HCl(aq) (1 mL). After addition of concentrated HCl(aq) (0.1 mL) air was passed through the mixture for 4 h. CHCl₃ was occasionally added to maintain the amount of the solution. The product was extracted with CHCl₃ several times, and the combined organic solution was dried over Na₂SO₄. After filtration the filtrate was concentrated and passed through an alumina plug (eluted with CH₂Cl₂). The yellow band was collected and purified by precipitation from CH₂Cl₂–pentane, and **24** was obtained as a pale yellow solid (126 mg, 0.127 mmol, 59% based on crude **22**; 21% based on Ru₃(CO)₁₂). ¹H NMR (C₆D₆): δ 7.04 (2H, s, Th), 1.70 (6H, s, Me–Th), 1.62, 1.43 (6H × 2, s × 2, C₅Me₄). IR (KBr): 2035, 1981 cm⁻¹. UV–vis (CH₂Cl₂): no characteristic absorption. FD–MS: 991 (M⁺), 936 (M⁺ – 2CO), 908 (M⁺ – 3CO), 879 (M⁺ – 4CO). Anal. Calcd for C₃₇H₃₂O₄F₆S₂Cl₂Ru₂: C, 44.81; H, 3.25. Found: C, 44.93; H, 3.49.

Preparation of 25. Crude **23** was chlorinated as described for the synthesis of **24** and obtained as a pale yellow solid (93% based on crude **23**; 74% based on Ru₃(CO)₁₂). ¹H NMR (C₆D₆): δ 7.38–7.27 (3H, m), 7.12–7.01 (3H, m), 6.92 (1H, s, Th), 1.73, 1.65 (3H × 2, s × 2, Me–Th), 1.55, 1.38 (6H × 2, s × 2, C₅Me₄). IR (KBr): 2036, 1982 cm⁻¹. UV–vis (CH₂Cl₂) λ_{max}/nm (ε/M⁻¹ cm⁻¹): 280 (2.65 × 10⁴), 258 (2.62 × 10⁴). FD–MS: 756 (M⁺). Anal. Calcd for C₃₂H₂₅FS₂ClRu: C, 50.83; H, 3.33. Found: C, 50.69; H, 3.46.

Photochromic Behavior of DTE–Ru Complexes. Photochromic behavior of the DTE–Ru complexes was monitored by ¹H NMR and UV–vis spectroscopy. As a typical example, the procedures for UV–vis monitoring of **24** (Figure 4b,c) are described, and other experiments were carried out in essentially the same manner. A CH₂Cl₂ solution of **24** (conc = 2.50 × 10⁻⁵ M) was prepared, and its UV–vis spectrum was recorded. Then the solution was placed at a distance of 10 cm from the UV lamp, and the intensity of the absorption at 556 nm was monitored by UV–vis spectroscopy at appropriate time intervals (Figure 4c). After 16 min the mixture reached the photostationary state, as can be seen from Figure 4b. Then the sample was placed at a distance of 6 cm from the Xe lamp, and the change was monitored by UV–vis spectroscopy; after 2 min the visible absorption completely disappeared. From the second cycle the absorption maxima observed after UV irradiation (16 min) and visible light irradiation (2 min) were monitored and plotted as shown in Figure 4c.

X-ray Crystallography. Single crystals were obtained by recrystallization from acetone–diethyl ether (**4**) and CH₂Cl₂–diethyl

ether (**11** and **24**) and mounted on glass fibers. Diffraction measurements were made on a Rigaku RAXIS IV imaging plate area detector with Mo K α radiation ($\lambda = 0.71069$ Å) at -60 °C. Indexing was performed from three oscillation images, which were exposed for 3 min. The crystal-to-detector distance was 110 mm ($2\theta_{\max} = 55^\circ$). In the reduction of data, Lorentz and polarization corrections and empirical absorption corrections were made.³² Crystallographic data and results of structure refinements are listed in Table 2.

The structural analysis was performed on an IRIS O2 computer using the teXsan structure solving program system obtained from the Rigaku Corp., Tokyo, Japan.³³ Neutral scattering factors were obtained from the standard source.³⁴

The structures were solved by a combination of the direct methods (SHELXS-86)³⁵ and Fourier synthesis (DIRDIF94).³⁶ Least-squares refinements were carried out using SHELXL-97³⁵ (refined on F^2) linked to teXsan. Unless otherwise stated, all non-

hydrogen atoms were refined anisotropically, and hydrogen atoms were fixed at the calculated positions. All three DTE derivatives were imposed on a crystallographic C_2 axis, and the F atoms of the hexafluorocyclopentene moieties were disordered and refined taking into account two components (F1,2:F1A,2A = 0.5:0.5; occupancy of F3,4 = 0.5). **4**: The disordered acetone solvate molecule was refined taking into account two components (O1–C42–C43:O1A–C42A–C43A = 0.766:0.234). **11**: The disordered F1,2 atoms were refined isotropically. The carbon atoms of the PPh₃ ligand were refined isotropically because of the small number of diffraction data with $I > 2\sigma(I)$. The disordered Cl atoms of the CH₂Cl₂ solvate molecule were also refined isotropically taking into account two components (Cl1,2:Cl1A,2A = 0.5:0.5).

Acknowledgment. This research was financially supported by the Ministry of Education, Culture, Sports, Science and Technology of the Japanese Government (Grant-in-Aid for Scientific Research on Priority Areas, No. 18065009, “Chemistry of Concerto Catalysis”), which is gratefully acknowledged. We are grateful to ZEON Corporation for a generous gift of perfluorocyclopentene **18**.

Supporting Information Available: Spectral changes of the DTE complexes upon UV and visible light irradiation and crystallographic results. This material is available free of charge via the Internet at <http://pubs.acs.org>.

OM700537S

(32) Higashi, T. *Program for Absorption Correction*; Rigaku Corp.: Tokyo, Japan, 1995.

(33) *teXsan; Crystal Structure Analysis Package, ver. 1. 11*; Rigaku Corp.: Tokyo, Japan, 2000.

(34) *International Tables for X-ray Crystallography*; Kynoch Press: Birmingham, 1975; Vol. 4.

(35) (a) Sheldrick, G. M. *SHELXS-86: Program for crystal structure determination*; University of Göttingen: Göttingen, Germany, 1986. (b) Sheldrick, G. M. *SHELXL-97: Program for crystal structure refinement*; University of Göttingen: Göttingen, Germany, 1997.

(36) Beurskens, P. T.; Admiraal, G.; Beurskens, G.; Bosman, W. P.; Garcia-Granda, S.; Gould, R. O.; Smits, J. M. M.; Smykalla, C. *The DIRDIF program system*, Technical Report of the Crystallography Laboratory; University of Nijmegen: Nijmegen, The Netherlands, 1992.